FULL PAPER

Luminescent 1,8-naphthalimide-derived Re(I) complexes: syntheses, spectroscopy, X-ray structure and preliminary bioimaging in fission yeast cells

Emily E. Langdon-Jones,[a] Catrin F. Williams,[b,c] Anthony J. Hayes,[c] David Lloyd,[c] Simon J. Coles,[d] Peter N. Horton,[d] Lara M. Groves,[a] and Simon J.A. Pope*[a]

Dedication ((optional))

Abstract: A series of picolyl-functionalised, fluorescent 1,8-naphthalimide ligands (L) have been synthesised and coordinated to Re(I) to form luminescent cationic complexes of the general form *fac*-[Re(phen)$(CO)_3$(L)]BF_4. The complexes were characterised using a range of spectroscopic techniques that confirm the proposed formulations. One example was characterised using X-ray crystallography revealing a distorted octahedral coordination sphere and Re-C/Re-N bond lengths in the expected ranges. All ligands were shown to be fluorescent, with the 4-amino derivatives showing intramolecular charge transfer. The complexes generally showed a mixture of ligand-centred and/or ^{3}MLCT emission depending upon the coordinated naphthalimide ligand. For selected complexes, confocal fluorescence microscopy was undertaken using fission yeast cells (*Schizosaccharomyces pombe*) and showed that the structure of the 1,8-naphthalimide ligand influences the uptake and localisation of the rhenium complex.

Introduction

The 1,8–naphthalimide structural motif is a remarkably functional moiety that has found utility in a wide variety of applications. Such derivatives can be synthesised in a stepwise manner allowing control over functionalisation. In particular, the electronic properties of substituted 1,8-naphthalimides have been utilized in a wide range of molecular architectures, from multichromophoric light harvesting arrays[1] to the design of fluorescent sensors[2] (for a multiplicity of analytes including, metal cations, anions, pH and biomolecules). 1,8-Naphthalimide based fluorophores are known to possess tuneable emission in the visible region (depending upon the nature and position of substituent), together with high photostability. For donor functionalized 1,8-naphthalimides, the nature of the emitting state is usually an intramolecular charge transfer (ICT), which results in solvatochromic behaviour. The fluorescence behaviour of such systems has been successfully applied to the design of probes for fluorescence cell imaging,[3] wherein high quantum yields and large Stokes' shifts are advantageous. Beyond their electronic properties, other very important uses for 1,8-naphthalimides include as DNA binding probes, [4] and as components of therapeutics (for example, amonafide[5]), including those with anticancer[6] properties. 1,8-Naphthalimides have also found far-ranging application in coordination chemistry, [7] including, for example, in the development of tyrosine kinase inhibitors,[8] lanthanide-based 3D supramolecular frameworks, [9] luminescent lanthanide assemblies,[10] and DNA-interacting organometallics.[11] In recent years we have studied the combination of 1,8-naphthalimide derived fluorophores with coordination complexes (e.g. with Au(I)) and investigated the resultant species in the context of cell imaging studies.[12] Following on from this work we present our findings on the development of mixed-ligand Re(I) complexes that incorporate a picolyl-functionalised 1,8-naphthalimide ligand. In recent years, organometallic Re(I) complexes have shown great utility in bioimaging studies using confocal fluorescence microscopy, [13] including examples which demonstrate ligand-derived control over intracellular localization. Herein, the synthesis and spectroscopic characterisation of a series of 1,8-naphthalimide functionalized ligands are described, together with their complexation to Re(I) to form complexes of the type *fac*-[Re(phen)$(CO)_3$(L)]BF_4 (where phen = 1,10-phenanthroline). Some preliminary cell imaging studies are also presented showing the applicability of such systems to bioimaging using fluorescence microscopy.

[a] Dr. E.E. Langdon-Jones, Dr. S.J.A. Pope
School of Chemistry
Cardiff University
Cardiff, UK CF10 3AT
E-mail:

[b] Dr. C.F. Williams
School of Engineering
Cardiff University
Cardiff, UK CF24 3AA

[c] Dr. C.F. Williams, Dr. A.J. Hayes, Prof. D. Lloyd
School of Biosciences
Cardiff University
Cardiff, UK CF10 3AT

[d] Dr. S.J. Coles, Dr. P.N. Horton
UK National Crystallographic Service, Chemistry, Faculty of Natural and Environmental Sciences, University of Southampton, Highfield, Southampton, SO17 1BJ England, UK

Supporting information for this article is given via a link at the end of the document.((Please delete this text if not appropriate))

Results and Discussion

Ligand synthesis and characterisation

Ligands (**L1–7**) were isolated, *via* one or two steps (Scheme 1), from commercially available 4-chloro-1,8-naphthalic anhydride. **L1** [14] has been previously reported. The first step involved conversion to 4- or 3-picolyl 4-chloro-substituted species (**L1–3**). **L2–3** could be further functionalised by substitution at the 4-position with either piperidine or benzylamine. Reaction was achieved by heating in DMSO at 70 °C with four equivalents of the respective amine. The successful formation of **L4–7** was easily determined by ^{1}H and $^{13}C\{^{1}H\}$ NMR spectroscopy. For **L6** and **L7** there was a characteristic N*H* resonance (broad triplet) at *ca*. 5.7 ppm. All ligands were characterised by high resolution mass spectrometry (HRMS) (ES^+), showing the $[M+H]^+$ cation peak in all cases. IR spectroscopy showed two C=O bands at *ca.* 1690 and 1650 cm^{-1}, with **L2–3** having an additional strong peak at *ca*. 780 cm^{-1} (C–Cl) and **L6–7**, with a secondary amine, showing the expected peaks for the N–H stretch and bend modes *ca.* 3300 and 1560 cm^{-1}.

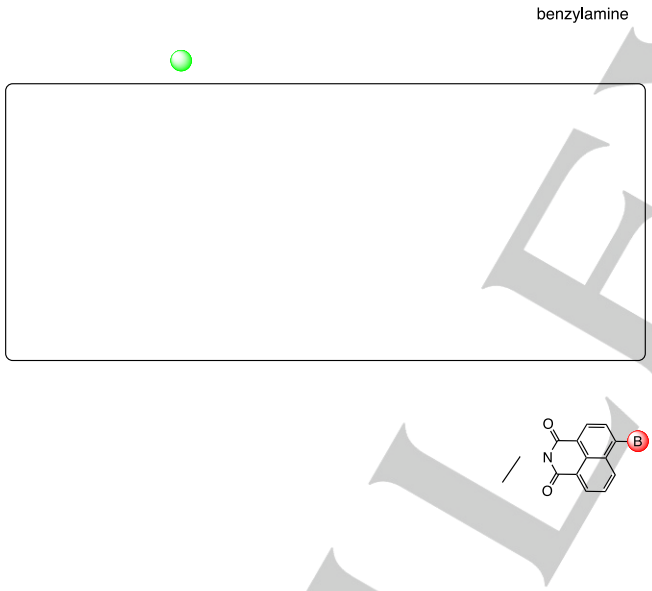

Scheme 1. Synthetic route to the ligands (shown inset) and complexes: (i) 3-picolylamine or 4-picolylamine, EtOH, heat; (ii) piperidine or benzylamine, DMSO, heat; (iii) 1,10-phenanthroline, toluene, heat; (iv) $AgBF_4$, MeCN; (v) L1-L7, $CHCl_3$, heat.

Complex Synthesis and Characterisation

The complexes were synthesised (Scheme 1) by heating *fac*-$[Re(CO)_3(phen)(MeCN)]BF_4$ with the appropriate ligand in chloroform under a dinitrogen atmosphere for 12 hours.[15] The Re(I) complexes were fully characterised by ^{1}H and $^{13}C\{^{1}H\}$ NMR, IR, UV-vis. spectroscopies and HRMS. ^{1}H NMR spectroscopy revealed a minor shift (*ca*. 0.2 ppm) of the N_{imide}–CH_2 resonance upon coordination to Re(I). $^{13}C\{^{1}H\}$ NMR spectroscopy distinguished the metal bound carbonyls (*ca.* 185-195 ppm) and ligand based C=O resonances (*ca.* 160 ppm). HRMS (ES^+) showed a cluster of peaks for the $[M]^+$ ion and also commonly $[M+MeCN]^+$. The presence of Re(I) was confirmed by the expected isotopic distribution (^{185}Re, 37.4%; ^{187}Re 62.6%). Furthermore, IR spectroscopy confirmed the proposed geometry with metal carbonyl stretches *ca*. 2030–1900 cm^{-1} and a slight shift in the imide carbonyl peaks at lower wavenumber values. IR spectroscopy data supported the assignment of an approximated C_{3v} or C_s symmetry at the complex, which predict either two or three carbonyl stretches for *fac*-$[Re(CO)_3(N^N)(X)]$ complexes. All complexes possessed an additional peak at *ca.* 1050 cm^{-1} assigned to the BF_4^- counter anion.

X-ray crystal structure of $[Re(phen)(CO)_3(L4)]BF_4$

A single crystal X-ray structure determination was obtained for *fac*-$[Re(phen)(CO)_3$(**L4**)$]BF_4$. Crystals were obtained via vapour diffusion of diethyl ether into a concentrated MeCN solution of the complex. The data collection parameters and refinement details are shown in Table S1; bond lengths and bond angles are shown in Table S2. The data analysis confirmed the proposed structure with a slightly distorted octahedral coordination geometry for rhenium, involving a *fac*–tricarbonyl arrangement combined with a chelating phenanthroline ligand and an axially N–coordinated **L4**. The bond lengths associated with the coordination sphere are typical of related Re(I) complexes.[16] The Re–CO distances lie within the range 1.875–1.948(XX) Å, whilst the Re–N distances were typically longer at 2.173–2.221 (XX) Å. It is noteworthy that the Re–N bond lengths to the axial monodentate pyridine are very similar to those associated with the chelating phenanthroline. This could be explained by the lack of distortion along the axial plane (C_{ax}–Re–N_{ax} 179.1(5)°) compared to the equatorial plane (C_{eqt}–Re–N_{eqt} 172.9(5)° and 175.0(5)°), resulting in a marginal strengthening of the Re–N_{py} bond and destabilisation of the Re–N_{phen} bond. Interestingly this example shows that the naphthalimide unit of **L4** is positioned over, and relatively co–planar to, the chelating phenanthroline ligand. However, this arrangement does not appear to be an intramolecular π–π stacking interaction (C_{naph}–C_{phen} 7.26–8.40 Å) and likely results from crystal packing effects.

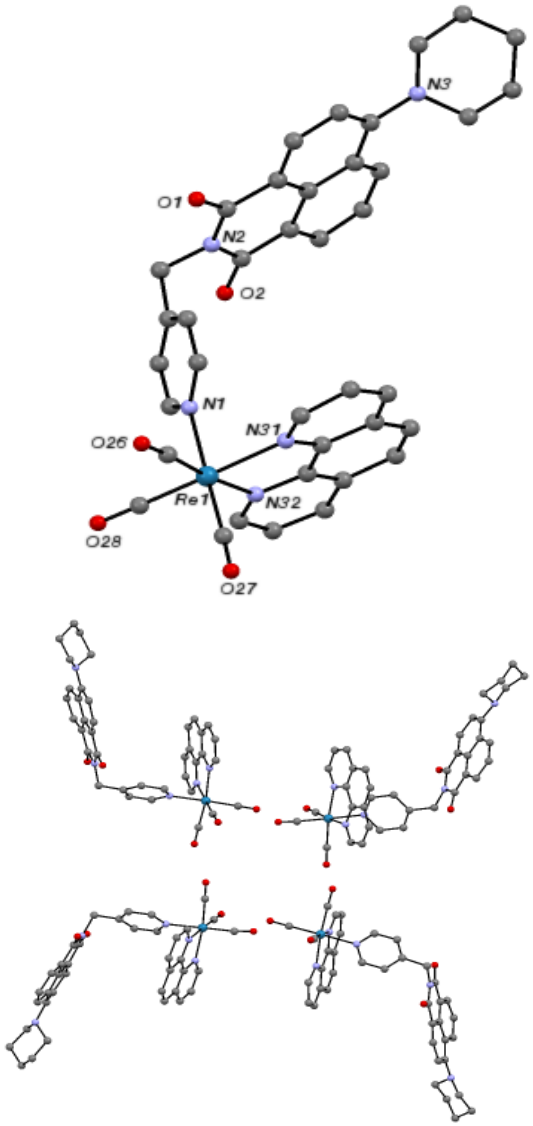

Figure 1. X-ray crystal structure of *fac*-[Re(phen)$(CO)_3$(L4)]BF_4 (top) with ellipsoids at 50 % occupancy, and (bottom) the crystal packing view of the complex. Counter anions and hydrogen atoms are omitted.

Electronic properties of the ligands and complexes

Table 1 shows the UV–vis. absorption properties of the free ligands and complexes. All ligands possessed strong π-π* bands below 350 nm (Fig. 2). For **L1–3**, the lowest energy peak is vibronically structured and associated with the naphthalimide core. The addition of the 4-amino substituent induced an additional unstructured band around 410–490 nm which is assigned to an intramolecular charge transfer (ICT), formally of n-π* character. The ICT band can be weakened by a lack of planarity between the naphthalimide ring and the 4-amino substituent. [17] The wavelength of the ICT absorption was bathochromically shifted for the benzylamine derivatives.

For all Re(I) complexes the absorption spectra were highly ligand dominated with the intense ICT transition overlapping with the anticipated $^1M_{Re}L_{phen}CT$ peak expected[18] of Re(I) phenanthroline complexes at 340–400 nm (*ca.* 10000 $M^{-1}cm^{-1}$). Furthermore the π-π* absorptions < 350 nm possessed higher molar absorption coefficients compared to the free ligands due to the summative effects of the phenanthroline and naphthalimide chromophores. The λ_{max} values for the latter show very little variation from the free ligands, presumably due to the lack of conjugation between the naphthalimide unit and the metal binding site.

Solutions of all ligands were found to be luminescent (Table 1). Measurements on aerated MeCN solutions of **L1–3** resulted in a faintly vibronically structured band between 380–410 nm (λ_{exc} = 345 nm), assigned to a ^{1}π-π* emitting state. For the amine-substituted naphthalimides, **L4–7**, each possessed a broad, unstructured emission band at 510-530 nm (Fig. 4 and Table 1). This band is more typical of a donor substituted naphthalimide species and consistent with an ICT character. The position of the ICT emission was dependent upon the nature of the 4-amino substituent, with the piperidine variants (**L4**, **L5**) giving the longest wavelength shift. The charge transfer nature of the emission band was exemplified by measuring in a range of solvents of different polarities whereupon the fluorophores demonstrated classical positive solvatochromism, as noted in our previous work.(REF gold paper) A comparison of the excitation spectra for the different types of ligands showed clear differences. For example, comparing **L2** and **L7** revealed very different excitation profiles with the latter showing a broad peak *ca*. 440 nm, which was assigned to the ICT transition and thus correlates relatively well with the observed ICT absorption band (*cf*. λ_{abs} = 428 nm). Emission lifetime data on **L1–7** showed that the ligands were fluorescent in all cases (confirming a singlet emitting excited state) with lifetimes ≤10 ns; it was noted that the benzylamine derivatives had the longest lifetimes in the series.

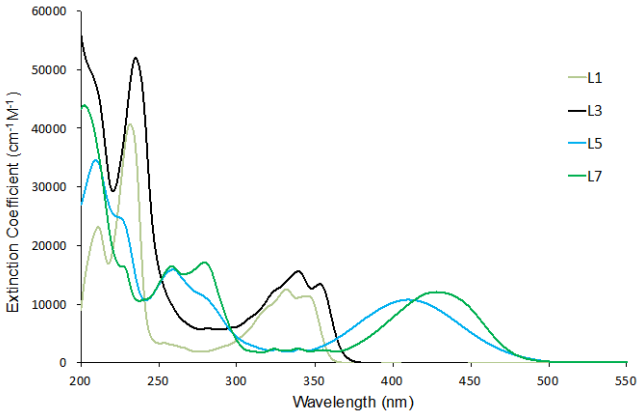

Figure 2. A comparison of the UV-vis. absorption spectra for **L1**, **L3**, **L5** and **L7**.

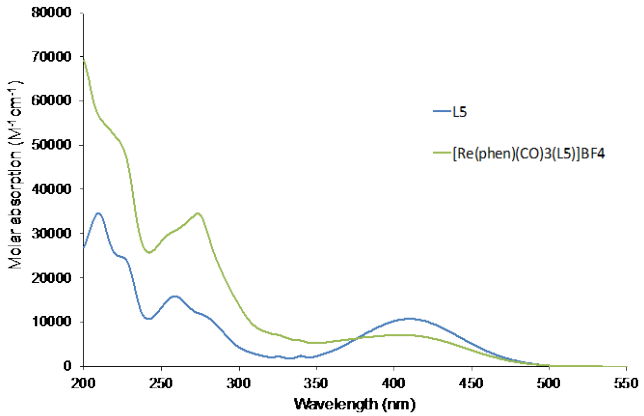

Figure 3. A comparison of the UV-vis. absorption spectra of **L5** and *fac*-[Re(phen)(CO)$_3$(**L5**)]BF$_4$.

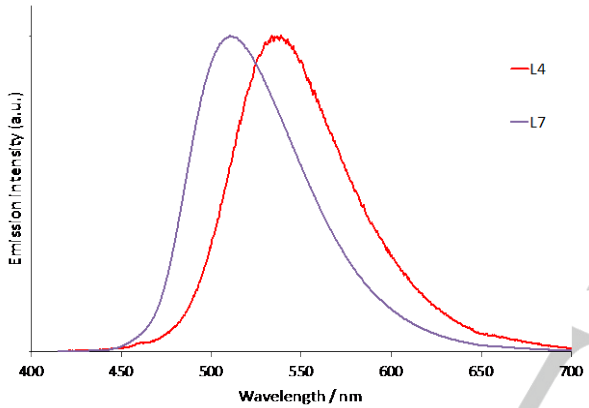

Figure 4. A comparison of the emission spectra (λ_{exc} = 405 nm) of **L4** (red) and **L7** (purple).

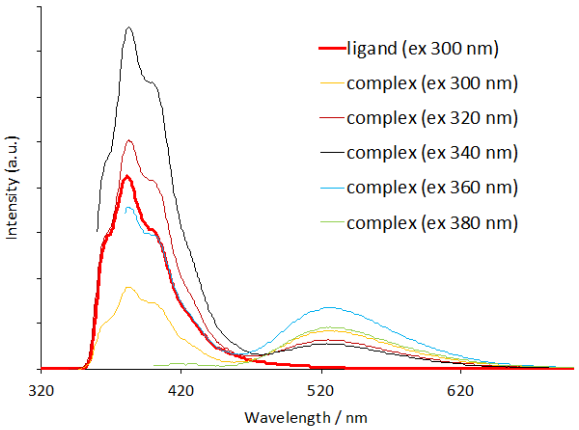

Figure 5. Emission spectra showing excitation wavelength dependence of *fac*-[Re(phen)(CO)$_3$(**L1**)]BF$_4$, together with a comparison to **L1** (red trace).

Table 1. Absorption and luminescence properties of the ligands and complexes.

Compound [a]	λ_{abs} / nm[b]	λ_{em} / nm[a, c]	τ / ns[d]
L1	344	381	<1
L2	340	392	9
L3	340	392	1
L4	411	534	<1
L5	410	534	<1
L6	429	512	10
L7	428	511	10
[Re(CO)$_3$(phen)(**L1**)]BF$_4$	345	528	190
[Re(CO)$_3$(phen)(**L2**)]BF$_4$	340	515	4, 40 (60%)
[Re(CO)$_3$(phen)(**L3**)]BF$_4$	340	515	8, 73 (75%)
[Re(CO)$_3$(phen)(**L4**)]BF$_4$	408	537	<1, 7 (51%)
[Re(CO)$_3$(phen)(**L5**)]BF$_4$	406	534	<1, 16 (66%)
[Re(CO)$_3$(phen)(**L6**)]BF$_4$	431	514	5, 10 (47%)
[Re(CO)$_3$(phen)(**L7**)]BF$_4$	431	511	<1, 10 (79%)

[a] MeCN; [b] only lowest energy absorption listed; [c] λ_{exc} = 425 nm, 5 × 10^{-5} M; [d] λ_{exc} = 295 or 459 nm;

For the complexes *fac*-[Re(phen)(CO)$_3$(**L1–3**)]BF$_4$ excitation at 405 nm gave a broad featureless peak *ca.* 515-528 nm. This excitation wavelength correlates with direct population of the ^{1}M$_{Re}$L$_{phen}$CT band since these complexes lack the naphthalimide-localised ICT character. Using higher energy excitation bands resulted in dual emission for all three complexes. For example, Fig. 5 shows the excitation wavelength dependent emission spectra for *fac*-[Re(phen)(CO)$_3$(**L1**)]BF$_4$. With comparison to **L1**, the vibronically structured emission peak at 340-440 nm can be attributed to naphthalimide-centred fluorescence, whilst the broad peak at 529 nm was assigned to the ^{3}M$_{Re}$L$_{phen}$CT transition. The corresponding lifetimes of these peaks confirm this assignment: with λ_{em} = 529 nm, the observed lifetime was 190 ns, which is consistent with cationic *fac*-[Re(phen)(CO)$_3$(L)]$^+$ type complexes, while at λ_{em} = 385 nm the lifetime was <10 ns.(REF) For *fac*-[Re(phen)(CO)$_3$(**L2**)]BF$_4$ and *fac*-[Re(phen)(CO)$_3$(**L3**)]BF$_4$ this ^{3}M$_{Re}$L$_{phen}$CT lifetime was shortened to 40 ns and 73 ns respectively, suggesting a partial quenching of the excited state possibly due to the nature of the axial ligand.

For the other complexes in the series there was a close correlation with the emission wavelengths of the corresponding free ligands. Lifetime measurements gave luminescence decay profiles that fitted best to a dual component biexponential, and the major contributions from these decays were <20 ns. This suggests that any ^{3}M$_{Re}$L$_{phen}$CT character is strongly quenched, due to the presence of the substituted naphthalimide ligands. This might be explained by the partial overlap of the ICT naphthalimide absorption band with the expected ^{3}M$_{Re}$L$_{phen}$CT emission profile. In the cases of the benzylamine variants *fac*-[Re(phen)(CO)$_3$(**L6**)]BF$_4$ and *fac*-[Re(phen)(CO)$_3$(**L7**)]BF$_4$, the

obtained lifetimes closely match those for the free ligands, suggesting 1,8-naphthalimide-dominated fluorescence emission for those species.

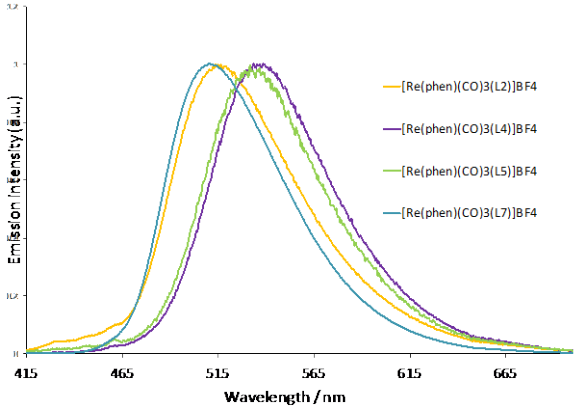

Figure 6. Comparison of the normalized emission spectra (λ_{exc} = 405 nm) of selected complexes.

Preliminary confocal fluorescence microscopy imaging with fission yeast

The calculated [19] water/octanol partition coefficients ($logP_{calc}$) were obtained for the free ligands showing that hydrophobicity increased across the series, **L1**($logP_{calc}$ = 2.42) < **L2**(2.99) < **L3**(3.05) < **L4**(3.33) < **L5**(3.38) < **L6**(3.57) < **L7**(3.62). These values predicted that addition of either piperidine or benzylamine substituents led to the most hydrophobic derivatives; enhanced lipophilicity is a common strategy for encouraging cellular uptake of a given agent. Preliminary confocal fluorescence microscopy was conducted on a selection of complexes to assess their prospective imaging capabilities. Complexes were incubated with fission yeast cells (*Schizosaccharomyces pombe*). Yeast cell walls typically allow translocation of compounds with molecular weights <1000 Da and were thus deemed suitable species for probing the fluorophores described herein. Cells were imaged using λ_{exc} = 405 nm and a detection wavelength window of 500-600 nm. Imaging was initially conducted with the 3-picolyl variants *fac*-[Re(phen)$(CO)_3$(**L**)]BF_4 species (where **L** = **L1**, **L3**, **L4**, **L5** and **L7**). Cells were incubated with the complexes at a concentration of 10 µg per mL, but resulted in very poor observed uptake. An increased probe concentration of 100 µg per mL generally resulted in much better uptake, although for *fac*-[Re(phen)$(CO)_3$(**L3**)]BF_4 uptake remained poor (only a handful of cells were stained), and both *fac*-[Re(phen)$(CO)_3$(**L4**)]BF_4 and *fac*-[Re(phen)$(CO)_3$(**L5**)]BF_4 showed evidence of precipitate formation at these higher concentrations. Even though uptake for *fac*-[Re(phen)$(CO)_3$(**L1**)]BF_4 (where emission was dominated by $^3M_{Re}L_{phen}CT$) was judged to be relatively modest, good quality cell images were still obtained (Fig. 7) showing uptake in both individual and dividing cells.

Of the complexes investigated in these bioimaging studies, the lipophilic benzylamine-substituted complex *fac*-[Re(phen)$(CO)_3$(**L7**)]BF_4 showed the best uptake. At 10 µg per mL incubation concentration, it showed some cytoplasmic staining and putative mitochondrial accumulation. At the higher incubation concentration, remarkably detailed images were collected that showed clear concentration of the compound in nuclei, particularly in dividing cells where two nuclei were present; cell division weakens the wall and membranes, enhancing their permeability and allowing uptake of the fluorophore.

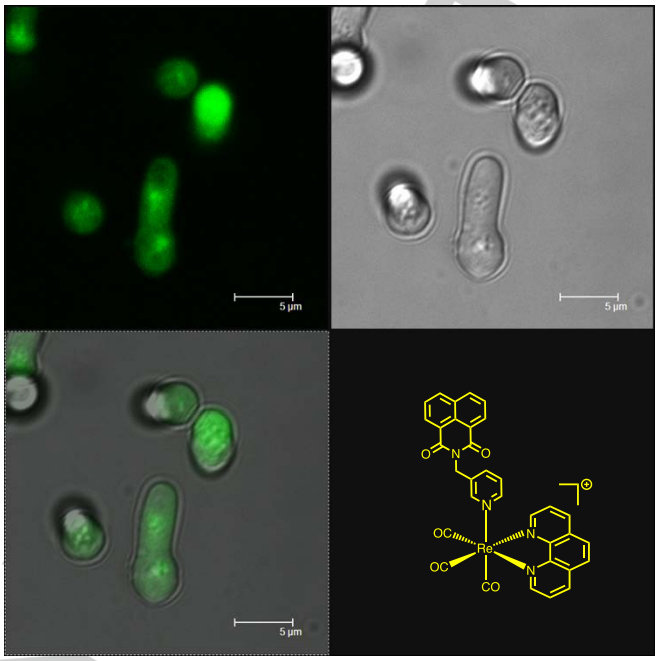

Figure 7. Confocal fluorescence microscopy of *S. pombe* yeast cells incubated with *fac*-[Re(phen)$(CO)_3$(**L1**)]BF_4 (λ_{exc} = 405 nm; λ_{em} = 500–600 nm) depicted in green; greyscale shows corresponding Nomarski D.I.C. transmitted light image. Scalebar in microns.

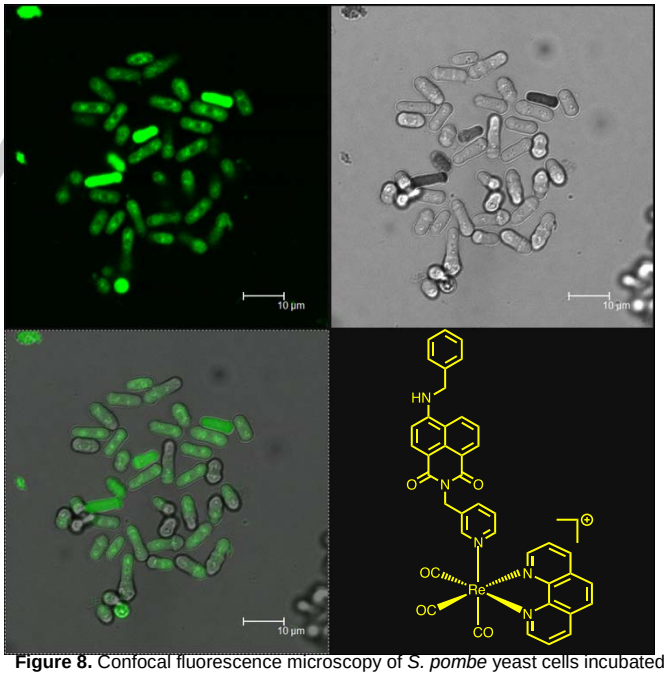

Figure 8. Confocal fluorescence microscopy of *S. pombe* yeast cells incubated with *fac*-[Re(phen)$(CO)_3$(**L7**)]BF_4 (λ_{exc} = 405 nm; λ_{em} = 500–600 nm) depicted in green; greyscale shows corresponding N omarski D.I.C. transmitted light image. Scalebar in microns.

Throughout the duration of the imaging experiments the populations of the cells were monitored with respect to an unstained control population. For *fac*-[Re(phen)$(CO)_3$(**L1**)]BF_4 the cell populations showed a very good stability perhaps reflecting the relatively poor uptake of this agent, whereas cells incubated with *fac*-[Re(phen)$(CO)_3$(**L7**)]BF_4 showed a 47% drop in population after 4 hrs. Both complexes also showed a degree of photobleaching which should be noted in future studies and may infer some phototoxicity.

Conclusions

Picolyl-derived ligands can be adorned with a range of naphthalimide derivatives to yield fluorescent species with tuneable emission. These ligands coordinate with Re(I) to give mixed ligand species of the form *fac*-[Re(phen)$(CO)_3$(L)]BF_4. The resultant complexes were characterized using a range of spectroscopic techniques and all were found to be luminescent. The origin of the luminescence, be it $^3M_{Re}L_{phen}CT$ or ligand-based, varies according to the nature of the specific naphthalimide ligand. A selection of complexes were chosen for cell imaging studies with fission yeast cells (*S. pombe*) and two examples were shown to be viable cell imaging agents. Uptake of the complexes appears to be modulated by the nature of the naphthalimide functionalisation, with the most lipophilic variant showing the best cell uptake.

Experimental Section

X-ray crystallography

Suitable crystals were selected and measured following a standard method[20] on a *Rigaku AFC12* goniometer equipped with an enhanced sensitivity (HG) *Saturn724+* detector mounted at the window of a *FR-E+ SuperBright* molybdenum rotating anode generator with HF *Varimax* optics (100µm focus) at 100K. Cell determination, data collection, reduction, cell refinement and absorption correction carried out using *CrystalClear-SM Expert 3.1b27*.[21]

The structures were solved by charge flipping using *SUPERFLIP*[22] and were completed by iterative cycles of ΔF-syntheses and full-matrix least squares refinement. All non-H atoms were refined anisotropically and difference Fourier syntheses were employed in positioning idealized hydrogen atoms and were allowed to ride on their parent C-atoms. It was not possible to accurately model the highly disordered solvent and thus PLATON SQUEEZE was used. Disorder was present in most of the BF4 counter ions resulting in the use of both geometrical (SAME) and thermal (SIMU) restraints. A general thermal restraint (DELU) was also used. All refinements were against F^2 and used *SHELXL-2014*.[23] Figures were created using the ORTEP3 software package. CCDC reference number 1443584 [Pt(L^3)(acac)] contains the supplementary crystallographic data for this paper. These data can be obtained free of charge from the Cambridge Crystallographic Data Centre *via* www.ccdc.cam.ac.uk/data_request/cif.

Cell incubation and confocal microscopy

The fission yeast *Schizosaccharomyces pombe* 972 h- was grown in 20 mL medium containing glucose (1%), peptone (1%), and yeast extract (0.3%) in Ehrlenmeyer flasks shaken at 30°C for 2 days, when glucose utilisation was complete. Washed once in PBS (phosphate-buffered saline, pH 7.4) after centrifugation at 1000 g for 2 min, they were incubated for 30 min with fluorophores in DMSO at 10 and 100 µg per mL (final concentrations in growth medium) at 20°C before washing again in PBS. Preparations were viewed by epifluorescence and transmitted light (Nomarski differential interference contrast optics) using a Leica TCS SP2 AOBS confocal laser scanning microscope (Leica, Germany) using ×63 or ×100 objectives, ×4 zoom factor and laser power of 20 %. Excitation of the fluorophore was at 405 nm using a 20 mW diode laser, with detection between 500–600 nm. In the majority of cases, initial imaging yielded minimal detectable fluorescence so the concentration of the fluorophore was increased to 100 µg per mL final concentration, which was then incubated with the cells at room temperature for a further 30 minutes.

General

^1H and ^{13}C-{^1H} NMR spectra were recorded on an NMR-FT Bruker 400 and 250 MHz spectrometer and recorded in $CDCl_3$. ^1H and $^{13}C\{^1H\}$ NMR chemical shifts (δ) were determined relative to residual solvent peaks with digital locking and are given in ppm. Low-resolution mass spectra were obtained by the staff at Cardiff University. High-resolution mass spectra were carried out at the EPSRC National Mass Spectrometry Facility at Swansea University. UV-Vis studies were performed on a Jasco V-570 spectrophotometer as MeCN solutions (2.5 or 5 × 10^{-5} M). Photophysical data were obtained on a JobinYvon–Horiba Fluorolog spectrometer fitted with a JY TBX picosecond photodetection module as MeCN solutions. Emission spectra were uncorrected and excitation spectra were instrument corrected. The pulsed source was a Nano-LED configured for 459 nm output operating at 1 MHz. Luminescence lifetime profiles were obtained using the JobinYvon–Horiba FluoroHub single photon counting module and the data fits yielded the lifetime values using the provided DAS6 deconvolution software.

All reactions were performed with the use of vacuum line and Schlenk techniques. Reagents were commercial grade and used without further purification. 4-Chloro-N-(4'-picolylamine)-1,8-naphthalimide (L1)[42] and *fac*-[Re(phen)$(CO)_3$(MeCN)]BF_4 were prepared according to the literature (REF).

Synthesis

Synthesis of 4-chloro-N-(4'-picolylamine)-1,8-naphthalimide **(L2)**

Prepared as for **L1(REF)** but using 4-chloro-1,8-naphthalic anhydride (1.997 g, 8.58 mmol) and 4-picolylamine (1.75 mL, 17.2 mmol) to give **L2** as a yellow solid (yield: 2.216 g, 80 %). ^1H NMR (250 MHz, $CDCl_3$): δ_H = 8.71–8.48 (m, 5H), 7.93–7.78 (m, 2H), 7.39 (d, 2H, $^3J_{HH}$ = 5.7 Hz), 5.37 (s, 2H, CH_2) ppm. UV–Vis (CH_3CN): λ_{max} ($\varepsilon/M^{-1}cm^{-1}$) = 353 (10800), 340 (12600), 235 (36300), 210 (20100) nm.

Synthesis of 4-chloro-N-(3'-picolylamine)-1,8-naphthalimide **(L3)**

Prepared as for **L1** but using 4-chloro-1,8-naphthalic anhydride (1.975 g, 8.49 mmol) and 3-picolylamine (1.75 mL, 17.2 mmol) to give **L3** as a yellow solid (yield: 2.444 g, 89 %). ^{1}H NMR (250 MHz, $CDCl_3$): δ_H = 8.76 (d, 1H, $^3J_{HH}$ = 1.4 Hz), 8.62–8.37 (m, 4H), 7.86–7.70 (m, 3H), 7.21–7.13 (m, 1H), 5.30 (s, 2H, CH_2) ppm. $^{13}C\{^1H\}$ NMR (300 MHz, $CDCl_3$): δ_C = 163.7 (CO), 163.5 (CO), 150.7, 149.0, 139.5, 137.1, 132.8, 132.4, 131.5, 131.0, 129.4, 127.9, 127.5, 123.5, 122.8, 121.3, 41.3 (CH_2) ppm. LRMS (ES^+) found m/z 323.06 for $[M+H]^+$, calculated 323.73 for $[M+H]^+$; HRMS (ES^+) found m/z = 323.0583, calculated 323.0582 for $[C_{18}H_{12}N_2O_2Cl]^+$. IR (solid) ν_{max} (±2 cm^{-1}) = 1697 (C=O), 1655 (C=O), 1616, 1590, 1570, 1505, 1478, 1462, 1400, 1373, 1339, 1316, 1234, 1225, 1173, 1159, 1117, 1094, 1053, 1028, 995, 955, 934, 912, 851, 793, 777 (C–Cl), 752, 733, 714, 667, 623 cm^{-1}. UV–Vis (CH_3CN): λ_{max} ($\varepsilon/M^{-1}cm^{-1}$) = 353 (13400), 340 (15600), 235 (52100) nm.

Synthesis of 4-piperidyl-N-(4'-picolylamine)-1,8-naphthalimide **(L4)**

L2 (104 mg, 0.32 mmol) and piperidine (0.13 mL, 1.29 mmol) were heated in DMSO (6 mL) under a dinitrogen atmosphere at 80 °C for 2 hours. The solution was allowed to cool and then water was added to induce precipitation of the product upon neutralisation with 1M HCl. The solution was then filtered and the solid washed with copious amounts of water, followed by petroleum ether, and subsequently dried *in vacuo* to give **L4** as a yellow solid (yield: 86 mg, 72 %). ^{1}H NMR (400 MHz, $CDCl_3$): δ_H = 8.52 (d, 1H, $^3J_{HH}$ = 7.3 Hz), 8.38–8.49 (m, 3H), 8.34 (d, 1H, $^3J_{HH}$ = 8.4 Hz), 7.68 (app t, 2H, $^3J_{HH}$ = 7.3 Hz), 7.63 (dd, 1H, J_{HH} = 8.4 Hz, 8.5 Hz), 7.32 (d, 2H, $^3J_{HH}$ = 5.9 Hz), 7.12 (d, 1H, $^3J_{HH}$ = 8.2 Hz), 5.30 (s, 2H, CH_2), 3.18 (t, 4H, $^3J_{HH}$ = 5.0 Hz, NCH_2), 1.87–1.72 (m, 4H, NCH_2CH_2) ppm. UV–Vis (CH_3CN): λ_{max} ($\varepsilon/M^{-1}cm^{-1}$) = 411 (10400), 339 (2000), 326 (1900), 275 (16000), 260 (17900), 225 (25000), 207 (33100) nm.

Synthesis of 4-piperidyl-N-(3'-picolylamine)-1,8-naphthalimide **(L5)**

Prepared as for **L4** using **L3** (100 mg, 0.31 mmol) and piperidine (0.06 mL, 0.62 mmol) however in this instance isolation of the pure product resulted from extraction of the neutralised reaction mixture into dichloromethane (2 × 20 mL). The organic layer was washed with water (3 × 20 mL), dried over $MgSO_4$ and reduced to a minimum volume. Precipitation of the product was then induced via the slow addition of petroleum ether. Subsequent filtration and drying *in vacuo* gave **L5** as an orange solid (yield: 111mg, 98 %). ^{1}H NMR (400 MHz, $CDCl_3$): δ_H = 8.81 (s, 1H), 8.53–8.47 (m, 2H), 8.43 (d, 1H, $^3J_{HH}$ = 8.2 Hz), 8.34 (d, 1H, $^3J_{HH}$ = 8.4 Hz), 8.19 (broad d, 1H, $^3J_{HH}$ = 7.9 Hz), 7.63 (dd, 1H, J_{HH} = 7.4, 7.3 Hz), 7.49–7.42 (m, 1H), 7.12 (d, 1H, $^3J_{HH}$ = 8.2 Hz), 5.37 (s, 1H, CH_2), 3.19 (t, 4H, $^3J_{HH}$ = 5.1 Hz, NCH_2), 1.88–1.79 (m, 4H, $NHCH_2CH_2$), 1.72–1.64 (m, 2H, $NCH_2CH_2CH_2$) ppm; $^{13}C\{^1H\}$ NMR (300 MHz, $CDCl_3$): δ_C = 164.6 (CO), 164.0 (CO), 157.7, 150.6, 148.8, 136.9, 133.3, 133.1, 131.4, 131.1, 130.0, 126.2, 125.4, 123.4, 122.8, 115.4, 114.8, 54.6, 41.0 (CH_2), 26.2, 24.3 ppm. LRMS (ES^+) found m/z = 372.17 for $[M+H]^+$; HRMS (ES^+) found m/z = 372.1706, calculated 372.1707 for $[C_{23}H_{22}N_2O_2]^+$. IR (solid) ν_{max} (±2 cm^{-1}) = 1688 (C=O), 1645 (C=O), 1584, 1570, 1512, 1481, 1449, 1429, 1414, 1377 (C–N), 1350, 1339, 1316, 1277, 1250, 1231, 1219, 1192, 1175, 1153, 1124, 1105, 1076, 1039, 1028, 985, 958, 939, 897, 864, 843, 814, 779, 758, 741, 712, 665 cm^{-1}. UV–Vis (CH_3CN): λ_{max} ($\varepsilon/M^{-1}cm^{-1}$) = 410 (10800), 340 (2500), 325 (2300), 259 (15900), 224 (24800), 209 (34600) nm.

Synthesis of 4-benzylamine-N-(4-picolylamine)-1,8-naphthalimide **(L6)**

Prepared as for **L5** but using **L2** (101 mg, 0.31 mmol) and benzylamine (0.10 mL, 0.62 mmol) in DMSO (4 mL), heating for 12 hours to give **L6** as a yellow–orange solid which was recrystallised from MeOH/ice cooled petroleum ether (yield: 122 mg, 94 %). ^{1}H NMR (400 MHz, $CDCl_3$): δ_H = 8.62 (d, 1H, $^3J_{HH}$ = 7.3 Hz), 8.52 (d, 1H, $^3J_{HH}$ = 5.7 Hz), 8.48 (d, 1H, $^3J_{HH}$ = 8.4 Hz), 8.17 (d, 1H, $^3J_{HH}$ = 8.5 Hz), 7.66 (t, 1H, $^3J_{HH}$ = 7.9 Hz), 7.55–7.33 (m, 7H), 6.80 (d, 1H, $^3J_{HH}$ = 8.5 Hz), 5.68 (t, 1H, $^3J_{HH}$ = 5.2 Hz, NH), 5.38 (s, 2H, NCH_2), 4.64 (d, 2H, $^3J_{HH}$ = 5.1 Hz, $NHCH_2$) ppm; $^{13}C\{^1H\}$ NMR (300 MHz, $CDCl_3$): δ_C = 164.6 (CO), 164.0 (CO), 149.8, 149.6, 146.8, 137.0, 135.0, 131.7, 130.4, 130.0, 129.2, 128.2, 127.7, 126.6, 125.1, 123.3, 122.7, 120.4, 110.3, 105.2, 48.1 ($NHCH_2$), 42.5 (CH_2) ppm. LRMS (ES^+) found m/z = 394.11 for $[M+H]^+$; HRMS (ES^+) found m/z = 394.1548, calculated 394.1550 for $[C_{25}H_{20}O_2N_3]^+$. IR (solid) ν_{max} (±2 cm^{-1}) = 3300 (N–H), 1684 (C=O), 1643 (C=O), 1574 (N–H bend), 1539, 1495, 1451, 1416, 1387, 1370, 1341, 1314, 1295, 1242, 1182, 1163, 1130, 1098, 1067, 1028, 991, 979, 963, 939, 772, 758, 737, 696, 669, 652, 633 cm^{-1}. UV–Vis (CH_3CN): λ_{max} ($\varepsilon/M^{-1}cm^{-1}$) = 429 (8100), 353 (3300), 339 (3800), 325 (3200), 279 (11600), 256 (11600), 229 (16100), 202 (36900) nm.

Synthesis of 4-benzylamine-(N-3-picolylamine)-1,8-naphthalimide **(L7)**

Prepared as for **L6** but using **L3** (174 mg, 0.54 mmol) and benzylamine (0.24 mL, 2.16 mmol) to give **L7** as an orange solid (yield: 90 mg, 42 %) ^{1}H NMR (400 MHz, $CDCl_3$): δ_H = 8.74 (s, 1H), 8.52 (d, 1H, $^3J_{HH}$ = 8.0 Hz), 8.36–8.42 (m, 2H), 8.06 (d, 1H, $^3J_{HH}$ = 8.5 Hz), 7.84–7.78 (m, 1H), 7.53 (dd, 1H, $^3J_{HH}$ = 7.5 Hz, $^3J_{HH}$ = 7.3 Hz), 7.39–7.24 (m, 5H), 7.18–7.11 (m, 1H), 6.68 (d, 1H, $^3J_{HH}$ = 8.5 Hz), 5.69 (t, 1H, $^3J_{HH}$ = 4.8 Hz, NH), 5.29 (s, 2H, CH_2), 4.54 (d, 2H, $^3J_{HH}$ = 5.1 Hz, $NHCH_2$) ppm; $^{13}C\{^1H\}$ NMR (300 MHz, $CDCl_3$): δ_C = 164.7 (CO), 164.0 (CO), 150.6, 149.5, 148.7, 136.9, 136.9, 134.9, 133.6, 131.6, 129.8, 129.2, 128.2, 127.7, 126.5, 125.0, 123.5, 122.9, 120.4, 110.4, 105.1, 48.1 ($NHCH_2$), 41.0 (CH_2) ppm. LRMS (ES^+) found m/z = 394.16 for $[M+H]^+$; HRMS (ES^+) found m/z = 394.1150, calculated 394.1150 for $[C_{25}H_{20}N_3O_2]^+$. IR (solid) ν_{max} (±2 cm^{-1}) = ca. 3350 (N–H), 1734, 1674 (C=O), 1630 (C=O), 1614, 1576 (N–H bend), 1559, 1516, 1497, 1479, 1451, 1429, 1393, 1369, 1344, 1318, 1298, 1236, 1221, 1186, 1163, 1132, 1120, 1103, 1096, 1065, 1043, 1030, 988, 970, 932, 856, 843, 816, 801, 769, 754, 714, 702, 669, 663 cm^{-1}. UV–Vis (CH_3CN): λ_{max} ($\varepsilon/M^{-1}cm^{-1}$) = 428 (12000), 356 (2100), 339 (2400), 324 (2300), 279 (17100), 258 (16400), 227 (16400), 202 (44000) nm.

Synthesis of *fac*-[Re(phen)$(CO)_3$(**L1**)]BF_4

fac-[Re(phen)$(CO)_3$(MeCN)]BF_4 (47 mg, 80.8 µmol) and **L1** (26 mg, 88.9 µmol) were dissolved in chloroform (3 mL) and heated at reflux, under a dinitrogen atmosphere, for 12 hrs. After cooling the solvent was reduced *in vacuo*. Precipitation of the product was then induced via the slow addition of diethyl ether. The product was subsequently filtered and dried *in vacuo* to give the product as an off-white solid (yield: 60.3 mg, 90 %). ^{1}H NMR (400 MHz, CD_3CN): δ_H = 9.45 (dd, 2H, J_{HH} = 5.4, 5.1 Hz), 8.92 (dd, 2H, J_{HH} = 8.3, 7.8 Hz), 8.76–8.73 (m, 1H), 8.60 (d, 2H, $^3J_{HH}$ = 7.3 Hz), 8.46 (d, 1H, $^3J_{HH}$ = 5.3 Hz), 8.40 (d, 2H, $^3J_{HH}$ = 8.2 Hz), 8.28 (s, 2H), 8.10 (dd, 2H, J_{HH} = 8.3, 5.1 Hz), 7.94–7.90 (m, 1H), 7.86 (t, 2H, $^3J_{HH}$ = 7.8 Hz), 7.38 (dd, 1H, J_{HH} = 8.2 Hz, 4.8 Hz), 5.36 (s, 2H, CH_2) ppm; $^{13}C\{^1H\}$ NMR (300 MHz, CD_3CN): very weak δ_C = 205.4 (M–CO), 161.5 (NCCO), 161.3 (NCCO), 154.6, 152.8, 150.2, 148.9, 140.1, 136.6, 134.5, 131.1, 128.0, 127.2, 125.6, 87.8 (CH_2) ppm. LRMS (ES^+) found m/z = 737.10 for $[M]^+$; HRMS (ES^+) found m/z = 737.0953, calculated 737.0598 for $[C_{33}H_{20}N_4O_5Re]^+$. IR (solid) ν_{max} (±2 cm^{-1}) = 2029 (C≡O), 1950 (C≡O), 1907 (C≡O), 1694 (C=O), 1655 (C=O), 1583, 1519, 1483, 1431, 1417, 1381, 1356, 1338, 1319, 1236, 1197, 1176, 1149, 1060, 1026, 974, 955, 935, 850, 810, 783, 771, 723, 710, 644, 624, 499, 420, 410 cm^{-1}. UV–Vis (CH_3CN): λ_{max} ($\varepsilon/M^{-1}cm^{-1}$) = 345 (14100), 332 (15900), 273 (43000), 230 (61600), 210 (46200), 202 (48200) nm.

Synthesis of *fac*-[Re(phen)$(CO)_3$(**L2**)]BF_4

Prepared as for *fac*-[Re(phen)(CO_3)(L1)]BF_4 using *fac*-[Re(phen)$(CO)_3$(MeCN)]BF_4 (31 mg, 53.6 µmol) and **L2** (19 mg, 59.0 µmol) to give *fac*-[Re(phen)(CO_3)(L2)]BF_4 as a yellow solid (yield: 31 mg, 68 %). ^{1}H NMR (400 MHz, $CDCl_3$): δ_H = 9.46 (dd, 2H, J_{HH} = 5.1, 3.8 Hz), 8.67 (d, 2H, $^3J_{HH}$ = 7.6 Hz), 8.43 (d, 1H, $^3J_{HH}$ = 8.5 Hz), 8.33 (d, 1H, $^3J_{HH}$ = 7.2 Hz), 8.17 (d, 1H, $^3J_{HH}$ = 7.9 Hz), 8.12–8.06 (m, 2H), 7.97 (s, 2H), 8.00–7.92 (m, 2H), 7.74–7.69 (m, 2H), 7.09 (d, 2H, $^3J_{HH}$ = 6.6 Hz), 4.99 (s, 2H, CH_2) ppm; $^{13}C\{^1H\}$ NMR (300 MHz, CD_3CN): δ_C = 163.4 (NCC=O), 163.2 (NCC=O), 154.5, 151.9, 150.8, 146.6, 140.3, 140.2, 138.8, 131.9, 131.3, 131.1, 130.8, 129.0, 128.8, 128.3, 128.1, 127.6, 127.1, 125.5, 122.6, 121.3, 118.2, 78.2, 42.1 (CH_2) ppm. LRMS (ES^+) found m/z = 773.21 for $[M]^+$; HRMS (FTMS) found m/z = 771.0567, calculated 771.0568 for $[ReC_{33}H_{19}N_4O_5Cl]^+$. IR (solid) ν_{max} (±2 cm^{-1}) = 2023 (C≡O), 1903 (C≡O), 1697 (C=O), 1654 (C=O), 1618, 1589, 1572, 1560, 1519, 1506, 1464, 1427, 1373, 1350, 1327, 1309, 1224, 1174, 1161, 1149, 1091, 1047, 1033, 960, 856, 815, 781, 754, 748, 723, 675, 659, 644 cm^{-1}. UV–Vis (CH_3CN): λ_{max} ($\varepsilon/M^{-1}cm^{-1}$) = 353 (16600), 340 (19700), 327 (17200), 274 (37000), 231 (67200), 213 (66400) nm.

Synthesis of *fac*-[Re(phen)$(CO)_3$(**L3**)]BF_4

Prepared as for *fac*-[Re(phen)(CO_3(L1)]BF_4 but using *fac*-[Re(phen)$(CO)_3$(MeCN)]BF_4 (38 mg, 65.9 µmol) and **L3** (25 mg, 73.2 µmol) to give *fac*-[Re(phen)(CO_3(L3)]BF_4 as a yellow solid (yield: 46 mg, 82 %). ^{1}H NMR (400 MHz, CD_3CN): δ_H = 9.42 (d, 2H, $^3J_{HH}$ = 3.6 Hz), 8.59–8.50 (m, 3H), 8.35 (dd, 1H, J_{HH} = 7.3 Hz, 1.0 Hz), 8.26 (d, 1H, $^3J_{HH}$ = 5.6 Hz), 8.20 (d, 2H, $^3J_{HH}$ = 7.9 Hz), 8.01 (d, 1H, $^3J_{HH}$ = 1.6 Hz), 7.92–7.81 (m, 7H), 7.07 (dd, 1H, J_{HH} = 7.8 Hz, 5.7 Hz), 4.83 (s, 2H, CH_2) ppm; $^{13}C\{^1H\}$ NMR (300 MHz, CD_3CN): δ_C = 195.7 (M–C≡O), 191.2 (M–C≡O), 163.2 (C=O), 163.0 (C=O), 154.5, 154.4, 152.0, 151.7, 146.5, 140.8, 140.2, 138.9, 136.0, 132.0, 131.2, 130.8, 129.1, 128.8, 128.4, 128.0, 127.7, 127.1, 126.2, 122.6, 121.3, 40.3 (CH_2) ppm. LRMS (ES^+) found m/z = 773.12 for $[M]^+$; HRMS (ES^+) found m/z = 771.0570, calculated 771.0568 for $[C_{33}H_{19}O_5N_4ClRe]^+$. IR (solid) ν_{max} (±2 cm^{-1}) = 2027 (C≡O), 1928 (C≡O), 1911 (C≡O), 1701 (C=O), 1666 (C=O), 1587, 1572, 1521, 1508, 1483, 1458, 1431, 1377, 1342, 1230, 1199, 1176, 1151, 1053, 1035, 850, 779, 752, 723, 706, 648 cm^{-1}. UV–Vis (CH_3CN): λ_{max} ($\varepsilon/M^{-1}cm^{-1}$) = 354 (16700), 340 (19600), 326 (17100), 274 (32200), 233 (62300), 211 (61000) nm.

Synthesis of *fac*-[Re(phen)$(CO)_3$(**L4**)]BF_4

Prepared as for *fac*-[Re(phen)(CO_3)(L1)]BF_4 using *fac*-[Re(phen)$(CO)_3$(MeCN)]BF_4 (40 mg, 69.2 µmol) and **L4** (28 mg, 76.1 µmol) to give the product as an orange–yellow solid (yield: 42 mg, 67 %). ^{1}H NMR (400 MHz, $CDCl_3$): δ_H = 9.50 (d, 2H, $^3J_{HH}$ = 4.6 Hz), 8.77 (d, 2H, $^3J_{HH}$ = 8.1 Hz), 8.34 (d, 1H, $^3J_{HH}$ = 6.6 Hz), 8.28 (t, 2H, $^3J_{HH}$ = 8.3 Hz), 8.28–8.16 (m, 6H), 7.55 (t, 1H, $^3J_{HH}$ = 7.5 Hz), 7.17 (d, 2H, $^3J_{HH}$ = 6.3 Hz), 7.04 (d, 1H, $^3J_{HH}$ = 8.2 Hz), 5.09 (s, 2H, CH_2), 3.15 (t, 4h, $^3J_{HH}$ = 4.6 Hz, NCH_2CH_2), 1.86–1.78 (m, 4H, NCH_2CH_2), 1.71–1.60 (m, 2H, $NCH_2CH_2CH_2$) ppm; $^{13}C\{^1H\}$ NMR (300 MHz, $CDCl_3$): δ_C = 195.1 (C≡O), 164.3 (C=O), 163.7 (C=O), 158.1, 154.3, 153.9, 152.0, 151.5, 151.3, 146.4, 140.6, 140.6, 133.4, 131.6, 131.4, 130.1, 128.6, 127.7, 126.1, 125,7, 125.4, 122.1, 114,8, 144.4, 52.5, 42.0, 26,1, 24.3 ppm. LRMS (ES^+) found m/z = 822.20 for $[M]^+$; HRMS (ES^+) found m/z = 820.1690, calculated 820.1693 for $[C_{38}H_{29}N_5O_5Re]^+$. IR (solid) ν_{max} (±2 cm^{-1}) = 2029 (C≡O), 1911 (C≡O), 1691, (C=O), 1654 (C=O), 1618, 1577, 1560, 1518, 1450, 1429, 1381, 1354, 1340, 1313, 1280, 1232, 1178, 1153, 1130, 1051, 1033, 989, 949, 914, 900, 848, 817, 760, 740, 723, 702, 671, 644, 624 cm^{-1}. UV–Vis (CH_3CN): λ_{max} ($\varepsilon/M^{-1}cm^{-1}$) = 408 (9700), 340 (5600), 326 (6600), 274 (36700) nm.

Synthesis of *fac*-[Re(phen)$(CO)_3$(**L5**)]BF_4

Prepared as for *fac*-[Re(phen)(CO_3)(L1)]BF_4 using *fac*-Re(phen)$(CO)_3$(MeCN)]BF_4 (39 mg, 67.4 µmol) and **L5** (31 mg, 74.1 µmol) to give the product as an orange solid (yield: 39 mg, 64 %). ^{1}H NMR (400 MHz, $CDCl_3$): δ_H = 9.54 (d, 2H, $^3J_{HH}$ = 4.6 Hz), 8.82–8.76 (m, 2H), 8.42–8.36 (m, 3H), 8.33 (d, 2H, $^3J_{HH}$ = 7.9 Hz), 8.10–8.01 (m, 5H), 7.96 (d, 1H, $^3J_{HH}$ = 7.9 Hz), 7.73 (t, 1H, $^3J_{HH}$ = 8.1 Hz), 5.02 (s, 2H, CH_2), 3.27 (broad t, 4H, NCH_2CH_2), 1.94–1.86 (m, 4H, NCH_2CH_2), 1.80–1.79 (m, 2H, $NCH_2CH_2CH_2$) ppm; $^{13}C\{^1H\}$ NMR (300 MHz, $CDCl_3$): δ_C = 195.3 (C≡O), 164.1 (C=O), 153.6, 153.1, 152.5, 152.3, 151.4, 146.3, 141.2, 140.6, 133.3, 131.8, 131.8, 131.4, 131.4, 128.6, 128.1, 127.5, 127.3, 126.9, 125.8, 125.7, 122.1, 54.8, 54.5, 40.0, 26.0, 24.1 ppm. LRMS (ES^+) found m/z = 822.24 for $[M]^+$; HRMS (ES^+) found m/z = 820.1691, calculated 820.1693 for $[C_{38}H_{29}N_5O_5Re]^+$. IR (solid) ν_{max} (±2 cm^{-1}) = 2031 (C≡O), 1911 (C≡O), 1691 (C=O), 1651 (C=O), 1585, 1519, 1483, 1431, 1417, 1381, 1346, 1317, 1280, 1234, 1199, 1178, 1151, 1057, 1035, 989, 989, 964, 947, 900, 875, 848, 785, 760, 740, 723, 706, 646, 628 cm^{-1}. UV–Vis (CH_3CN): λ_{max} ($\varepsilon/M^{-1}cm^{-1}$) = 406 (7000), 274 (34500) nm.

Synthesis of *fac*-[Re(phen)$(CO)_3$(**L6**)]BF_4

Prepared as for *fac*-[Re(phen)(CO_3)(L1)]BF_4 but using *fac*-[Re(phen)$(CO)_3$(MeCN)]BF_4 (38 mg, 65.7 µmol) and **L6** (27 mg, 72.3 µmol) to give the product as a yellow solid (yield: 42 mg, 61 %). ^{1}H NMR (250 MHz, CD_3CN): δ_H = 9.60 (d, 2H, $^3J_{HH}$ = 5.13 Hz), 8.81 (dd, 2H, J_{HH} = 7.6, 7.9 Hz), 8.40 (t, 2H, $^3J_{HH}$ = 7.8 Hz), 8.24–8.06 (m, 8H), 7.65 (t, 1H, $^3J_{HH}$ = 8.1 Hz), 7.51–7.32 (m, 4H), 7.18 (d, 2H, $^3J_{HH}$ = 7.4 Hz), 6.98 (t, 1H, 5.3 Hz, NH), 6.62 (d, 1H, $^3J_{HH}$ = 8.0 Hz), 5.10 (s, 2H, NCH_2), 4.68 (d, 2H, $^3J_{HH}$ = 6.0 Hz, $NHCH_2$) ppm; $^{13}C\{^1H\}$ NMR (300 MHz, CD_3CN): δ_C = 195.5 (C≡O), 191.5 (C≡O), 164.2 (C=O), 163.1 (C=O), 154.7, 151.7, 150.3, 146.6, 140.3, 138.2, 134.1, 131.3, 131.0, 128.7, 128.1, 127.9, 127.4, 127.2, 127.1, 125.4, 124.7, 122.1, 120.3, 108.8, 104.8, 46.43 (CH_2), 41.6 ($NHCH_2$) ppm. LRMS (ES^+) found m/z = 844.24 for $[M]^+$; HRMS found m/z = 842.1536, calculated 842.1536 for $[C_{40}H_{27}N_5O_5Re]^+$. IR (solid) ν_{max} (±2 cm^{-1}) = 2031 (C≡O), 1913 (C≡O), 1685 (C=O), 1647 (C=O), 1618, 1577, 1550, 1521, 1503, 1496, 1429, 1392, 1369, 1356, 1344, 1315, 1296, 1246, 1184, 1166, 1136, 1057, 1053, 993, 943, 918, 877, 848, 817, 802, 775, 758, 742, 723, 698, 645, 628 cm^{-1}. UV–Vis (CH_3CN): λ_{max} ($\varepsilon/M^{-1}cm^{-1}$) = 431 (14600), 354 (6900), 337 (9300), 323 (9600), 275 (47300), 256 (39800), 226 (58400) nm.

Synthesis of *fac*-[Re(phen)$(CO)_3$(L7)]BF_4

Prepared as for *fac*-[Re(phen)(CO_3)(L1)]BF_4 but using *fac*-[Re(phen)$(CO)_3$(MeCN)]BF_4 (42 mg, 72.1 µmol) and L7 (31 mg, 79.3 µmol) to give the product as a yellow solid (yield: 43 mg, 64 %). ^{1}H NMR (400 MHz, CD_3CN): δ_H = 9.39 (d, 2H, $^3J_{HH}$ = 3.8 Hz), 8.44 (m, 2H), 8.32 (d, 2H, $^3J_{HH}$ = 4.9 Hz), 8.29 (d, 2H, $^3J_{HH}$ = 8.2 Hz), 8.02 (d, 1H, $^3J_{HH}$ = 8.6 Hz), 7.83 (s, 1H), 7.82–7.71 (m, 5H), 7.66 (t, 1H, $^3J_{HH}$ = 7.9 Hz), 7.51 (s, 1H), 7.41 (d, 2H, $^3J_{HH}$ = 7.5 Hz), 7.31 (t, 2H, $^3J_{HH}$ = 7.5 Hz), 7.11 (dd, 1H, J_{HH} = 7.7 Hz, 5.6 Hz), 7.02 (app s, 1H, N*H*), 6.66 (d, 1H, $^3J_{HH}$ = 8.6 Hz), 4.83 (s, 2H, CH_2), 4.66 (d, 2H, $^3J_{HH}$ = 6.0 Hz, $NHCH_2$) ppm; $^{13}C\{^1H\}$ NMR (300 MHz, CD_3CN): δ_C = 195.7 (C≡O), 191.5 (C≡O), 163.8 (C=O), 162.9 (C=O), 154.3, 151.7, 150.5, 146.3, 140.3, 139.9, 140.0, 138.3, 137.0, 134.3, 131.2, 131.0, 129.7, 128.7, 128.0, 127.8, 127.4, 127.3, 126.9, 126.1, 124.9, 122.1, 120.7, 120.6, 119.9, 119.1, 105.0, 46.5 (CH_2), 39.9 ($NHCH_2$) ppm. LRMS (ES^+) found *m/z* = 844.16 for $[M]^+$; HRMS (FTMS) found *m/z* 842.1543 for $[C_{40}H_{27}N_5O_5Re]^+$, calculated 842.1536 for

$[C_{40}H_{27}N_5O_5Re]^+$. IR (solid) ν_{max} (±2 cm^{-1}) = 2031 (C≡O), 1915 (C≡O), 1683 (C=O), 1645 (C=O), 1602, 1577, 1548, 1494, 1471, 1446, 1419, 1390, 1369, 1346, 1317, 1296, 1246, 1182, 1165, 1136, 1060, 1033, 939, 908, 898, 802, 771, 734, 702, 646, 628 cm^{-1}. UV–Vis (CH_3CN): λ_{max} (ε/$M^{-1}cm^{-1}$) = 431 (16500), 323 (8300), 275 (47800), 257 (40800), 226 (53500) nm.

Acknowledgements

We thank Cardiff University for financial support and the staff of the EPSRC Mass Spectrometry National Service (University of Swansea) for providing MS data and the EPSRC UK National Crystallographic Service at the University of Southampton.

Keywords: fluorescence • cell imaging • rhenium • naphthalimide

[1] For example, N.I. Georgiev, V.B. Bojinov, M. Marinova, *Sens. Act. B*. **2010**, *150*, 655; N.I. Georgiev, V.B. Bojinov, *Dyes Pigm*. **2010**, *84*, 249; V.B. Bojinov, N.I. Georgiev, P.S. Nikolov, *J. Photochem. Photobiol. A* **2008**, *197*, 281; A.M.M. El-Betany, L. Vachova, C.G. Bezzu, S.J.A. Pope, N.B. McKeown, *Tetrahedron* **2013**, *69*, 8439; C. Felip-Leon, S. Diaz-Oltra, F. Galindo, J.F. Miravet, *Chem. Mat*. **2016**, *28*, 7964; R.K. Dubey, D. Inan, S. Sengupta, E.J.R. Sudholter, F.C. Grozema, W.F. Jager, Chem. Sci. 2016, 7, 3517; C-C. You, C. Hippius, M. Grune, F. Wurthner, Chem. Eur. J. 2006, 12, 7510

[2] R.M. Duke, E.B. Veale, F.M. Pfeffer, P.E. Kruger, T. Gunnlaugsson, Chem. Soc. Rev. 2010, 39, 3936

[3] E. Calatrava, S.A. Bright, S. Achermann, C. Moylan, M.O. Senge, E.B. Veale, D.C. Williams, T. Gunnlaugsson, E.M. Scanlan, Chem. Commun. 2016, 52, 13086; S-A. Choi, C.S. Park, O.S. Kwon, H-K. Giong, J-S. Lee, T.H. Ha, C-S. Lee, *Sci. Rep*. **2016**, *6*, 26203; C. Satriano, G.T. Sfrazzetto, M.E. Amato, F.P. Ballistreri, A. Copani, M.L. Giuffrida, G. Grasso, A. Pappalardo, E. Rizzarelli, G.A. Tomaselli, R.M. Toscano, Chem. Commun. 2013, 49, 5565; Y. Dai, B-K. Lv, X-F. Zhang, Y. Xiao, Chin. Chem. Lett. 2014, 25, 1001; L. Zhang, F. Su, X. Kong, F. Lee, S. Sher, K. Day, Y. Tian, D.R. Meldrum, ChemBioChem 2016, 17, 1719

[4] M.J. Waring, A. Gonzalez, A. Jimenez, D. Vazquez, Nucl. Acid Res. 1979, 7, 217; B.S. Andersson, M. Beran, N. Bakic, L.E. Silbermann, R.A. Newman, Cancer Res. 1987, 47, 1040; K.A. Stevenson, S.F. Yen, N.C. Yang, D.W. Boykin, W.D. Wilson, J. Med. Chem. 1084, 27, 1677; R.K.Y. Zee-Cheng, C.C. Cheng, J. Med. Chem. 1985, 28, 1216

[5] G. Gellerman, Lett. Drug Des. Disc. 2016, 13, 47

[6] For example, M. Lv, H. Xu, Curr. Med. Chem. 2009, 16, 4797; L. Ingrassia, F. Lefranc, R. Kiss, T. Mijatovic, Curr. Med. Chem. 2009, 16, 1192; Z. Chen, X. Liang, H. Zhang, H. Xie, J. Liu, Y. Xu, W. Zhu, Y. Wang, X. Wang, S. Tan, D. Kuang, X. Qian, J. Med. Chem. 2010, 53, 2589; A. Wu, Y. Xu, X. Qian, J. Wang, J. Liu, Eur. J. Med. Chem. 2009, 44, 4674; A. Wu, Y. Xu, X. Qian, Bioorg. Med. Chem. 2009, 17, 592

[7] S. Banerjee, E.B. Veale, C.M. Phelan, S.A. Murphy, G.M. Tocci, L.J. Gillespie, D.O. Frimannsson, J.M. Kelly, T. Gunnlaugsson, *Chem. Soc. Rev*. **2013**, *42*, 1601

[8] S. Tan, K. Han, Q. Li, L. Tong, Y. Yang, Z. Chen, H. Xie, J. Ding, X. Qian, Y. Xu, Eur. J. Med. Chem. 2014, 85, 207

[9] D.L. Reger, A. Leitner, M.D. Smith, Cryst. Growth Des. 2015, 15, 5637

[10] V.F. Plyusnin, A.S. Kupryakov, V.P. Grivin, A.H. Shelton, I.V. Sazanovich, A.J.H.M. Meijer, J.A. Weinstein, M.D. Ward, Photochem. Photobiol. Sci. 2013, 12, 1666; A.H. Shelton, I.V. Sazanovich, J.A. Weinstein, M.D. Ward, Chem. Commun. 2012, 48, 2749

[11] W. Streciwilk, A. Terenzi, R. Misgeld, C. Frias, P.G. Jones, A. Prokop, B.K. Keppler, I. Ott, ChemMedChem 2017, 12, 214; J.M. Perez, I. Lopez-Solera, E.I. Montero, M.F. Brana, C. Alonso, S.P. Robinson, C.J. Navarro-Ranninger, J. Med. Chem. 1999, 42, 5482; S. Banerjee, J.A. Kitchen, S.A. Bright, J.E. O'Brien, D.C. Williams, J.M. Kelly, T. Gunnlaugsson, T. Chem. Commun. 2013, 49, 8522; C.P. Bagowski, Y. You, H. Scheffler, D.H. Vlecken, D. J. Schmitz, I. Ott, Dalton Trans. 2009, 10799; K.J. Kilpin, C.M. Clavel, F. Edafe, P.J. Dyson, Organometallics 2012, 31, 7031; J.M. Perez, I. Lopez-Solera, E.I. Montero, M.F. Brana, C. Alonso, S.P. Robinson, C. Navarro-Ranniger, J. Med. Chem. 1999, 42, 5482; S. Roy, S. Saha, R. Mujumdar, R.R. Dighe, A.R. Chakravarty, Inorg. Chem. 2009, 48, 9501

[12] E.E. Langdon-Jones, D. Lloyd, A.J. Hayes, S.D. Wainwright, H.J. Mottram, S.J. Coles, P.N. Horton, S.J.A. Pope, *Inorg. Chem*. **2015**, *54*, 6606; E.E. Langdon-Jones, N.O. Symonds, S.E. Yates, A.J. Hayes, D. Lloyd, R. Williams, S.J. Coles, P.N. Horton, S.J.A. Pope, *Inorg. Chem*. **2014**, *53*, 3788

[13] For example, A.J. Amoroso, M.P. Coogan, J.E. Dunne, V. Fernandez-Moreira, J.B. Hess, A.J. Hayes, D. Lloyd, C. Millet, S.J.A. Pope, C. Williams, Chem. Commun. 2007, 3066; A.W-T. Choi, M-W. Louie, S.P-Y. Li, H-W. Liu, B.T-N. Chan, T.C-Y. Lam, A.C-C. Lin, S-H. Cheng, K.K-W. Lo, Inorg. Chem. 2012, 51, 13289; A. Palmioli, A. Aliprandi, D. Septiadi, M. Mauro, A. Bernardi, L. De Cola, M. Panigati, Org. Biomol. Chem. 2017, 15, 1686; V. Fernandez-Moreira, M.L. Ortego, C.F. Williams, M.P. Coogan, M. D. Villacampa, M.C. Gimeno, Organometallics 2012, 31, 5950; E.E. Langdon-Jones, A.B. Jones, C.F. Williams, A.J. Hayes, D. Lloyd, H.J. Mottram, S.J.A. Pope, Eur. J. Inorg. Chem. 2017, 759; R.G. Balasingham, F.L. Thorp-Greenwood, C.F. Williams, M.P. Coogan, S.J.A. Pope, Inorg. Chem. 2012, 51, 1419; A.J. Amoroso, R.J. Arthur, M.P. Coogan, J.B. Court, V. Fernandez-Moreira, A.J. Hayes, D. Lloyd, C. Millet, S.J.A. Pope, New J. Chem. 2008, 32, 1097

[14] K. de Oliveira, P. Costa, J. Santin, L. Mazzambani, C. Burger, C. Mora, R. Nunes, M. de Souza, Bioorg. Med. Chem. 2011, 19, 4295

[15] L.A. Mullice, S.J.A. Pope, Dalton Trans. 2010, 39, 5908

[16] F.L. Thorp-Greenwood, M.P. Coogan, A.J. Hallett, R.H. Laye, S.J.A. Pope, J. Organomet. Chem. 2009, 694, 1400

[17] Z.Y. Wu, J.N. Cui, X.H. Xian, T.Y. Liu, Chin. Chem. Lett. 2013, 24, 359

[18] M. Wrighton, D.L. Morse, J. Am. Chem. Soc. 1974, 96, 998

[19] http://www.molinspiration.com

[20] S.J. Coles, P.A. Gale, *Chem. Sci*. 2012, **3**, 683

[21] *CrystalClear-SM Expert 3.1 b27*, 2013, Rigaku

[22] L. Palatinus, G. Chapuis, *J. Appl. Cryst*. 2007, **40**, 786

[23] G.M. Sheldrick, *Acta Cryst*. 2015, **C71**, 3

[24]

[25]

[26]

[27]

[28]

[29]

[30]

[31]

[32]

[33]

[34]

[35]

[36]

[37]

[38]

[39]

[40]

Entry for the Table of Contents (Please choose one layout)

Layout 1:

FULL PAPER

1,8-Naphthalimide-derived, picolyl-based ligands have been coordinated to Re(I) to form luminescent complexes. The complexes were characterized using an array of spectroscopic methods and one example provided an X-ray crystal structure. Selected complexes were explored as fluorescence cell imaging agents using fission yeast cells.

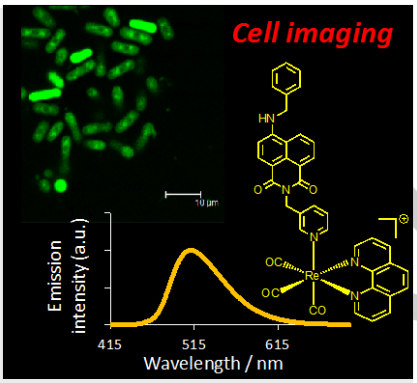

*Emily E. Langdon-Jones, Catrin F. Williams, Anthony J. Hayes, David Lloyd, Simon J. Coles, Peter N. Horton, Lara M. Groves, and Simon J.A. Pope**

Page No. – Page No.
Luminescent 1,8-naphthalimide-derived Re(I) complexes: syntheses, spectroscopy, X-ray structure and preliminary bioimaging in fission yeast cells

Layout 2:

FULL PAPER

((Insert TOC Graphic here; max. width: 11.5 cm; max. height: 2.5 cm))

*Author(s), Corresponding Author(s)**

Page No. – Page No.

Title

Text for Table of Contents

[1] For example, N.I. Georgiev, V.B. Bojinov, M. Marinova, Sens. Act. B. 2010, 150, 655; N.I. Georgiev, V.B. Bojinov, Dyes Pigm. 2010, 84, 249; V.B. Bojinov, N.I. Georgiev, P.S. Nikolov, J. Photochem. Photobiol. A 2008, 197, 281; A.M.M. El-Betany, L. Vachova, C.G. Bezzu, S.J.A. Pope, N.B. McKeown, Tetrahedron 2013, 69, 8439; C. Felip-Leon, S. Diaz-Oltra, F. Galindo, J.F. Miravet, Chem. Mat. 2016, 28, 7964; R.K. Dubey, D. Inan, S. Sengupta, E.J.R. Sudholter, F.C. Grozema, W.F. Jager, Chem. Sci. 2016, 7, 3517; C-C. You, C. Hippius, M. Grune, F. Wurthner, Chem. Eur. J. 2006, 12, 7510
[2] R.M. Duke, E.B. Veale, F.M. Pfeffer, P.E. Kruger, T. Gunnlaugsson, Chem. Soc. Rev. 2010, 39, 3936.
[3] E. Calatrava, S.A. Bright, S. Achermann, C. Moylan, M.O. Senge, E.B. Veale, D.C. Williams, T. Gunnlaugsson, E.M. Scanlan, Chem. Commun. 2016, 52, 13086; S-A. Choi, C.S. Park, O.S. Kwon, H-K. Giong, J-S. Lee, T.H. Ha, C-S. Lee, *Sci. Rep*. **2016**, *6*, 26203; C. Satriano, G.T. Sfrazzetto, M.E.

Amato, F.P. Ballistreri, A. Copani, M.L. Giuffrida, G. Grasso, A. Pappalardo, E. Rizzarelli, G.A. Tomaselli, R.M. Toscano, Chem. Commun. 2013, 49, 5565; Y. Dai, B-K. Lv, X-F. Zhang, Y. Xiao, Chin. Chem. Lett. 2014, 25, 1001; L. Zhang, F. Su, X. Kong, F. Lee, S. Sher, K. Day, Y. Tian, D.R. Meldrum, ChemBioChem 2016, 17, 1719

[4] M.J. Waring, A. Gonzalez, A. Jimenez, D. Vazquez, Nucl. Acid Res. 1979, 7, 217; B.S. Andersson, M. Beran, N. Bakic, L.E. Silbermann, R.A. Newman, Cancer Res. 1987, 47, 1040; K.A. Stevenson, S.F. Yen, N.C. Yang, D.W. Boykin, W.D. Wilson, J. Med. Chem. 1084, 27, 1677; R.K.Y. Zee-Cheng, C.C. Cheng, J. Med. Chem. 1985, 28, 1216;

[5] G. Gellerman, Lett. Drug Des. Disc. 2016, 13, 47.

[6] For example, M. Lv, H. Xu, Curr. Med. Chem. 2009, 16, 4797; L. Ingrassia, F. Lefranc, R. Kiss, T. Mijatovic, Curr. Med. Chem. 2009, 16, 1192; Z. Chen, X. Liang, H. Zhang, H. Xie, J. Liu, Y. Xu, W. Zhu, Y. Wang, X. Wang, S. Tan, D. Kuang, X. Qian, J. Med. Chem. 2010, 53, 2589; A. Wu, Y. Xu, X. Qian, J. Wang, J. Liu, Eur. J. Med. Chem. 2009, 44, 4674; A. Wu, Y. Xu, X. Qian, Bioorg. Med. Chem. 2009, 17, 592;

[7] S. Banerjee, E.B. Veale, C.M. Phelan, S.A. Murphy, G.M. Tocci, L.J. Gillespie, D.O. Frimannsson, J.M. Kelly, T. Gunnlaugsson, *Chem. Soc. Rev.* **2013**, *42*, 1601

[8] S. Tan, K. Han, Q. Li, L. Tong, Y. Yang, Z. Chen, H. Xie, J. Ding, X. Qian, Y. Xu, Eur. J. Med. Chem. 2014, 85, 207;

[9] D.L. Reger, A. Leitner, M.D. Smith, Cryst. Growth Des. 2015, 15, 5637

[10] V.F. Plyusnin, A.S. Kupryakov, V.P. Grivin, A.H. Shelton, I.V. Sazanovich, A.J.H.M. Meijer, J.A. Weinstein, M.D. Ward, Photochem. Photobiol. Sci. 2013, 12, 1666; A.H. Shelton, I.V. Sazanovich, J.A. Weinstein, M.D. Ward, Chem. Commun. 2012, 48, 2749.

[11] W. Streciwilk, A. terenzi, R. Misgeld, C. Frias, P.G. Jones, A. Prokop, B.K. Keppler, I. Ott, ChemMedChem 2017, 12, 214; J.M. Perez, I. Lopez-Solera, E.I. Montero, M.F. Brana, C. Alonso, S.P. Robinson, C.J. Navarro-Ranninger, J. Med. Chem. 1999, 42, 5482; S. Banerjee, J.A. Kitchen, S.A. Bright, J.E. O'Brien, D.C. Williams, J.M. Kelly, T. Gunnlaugsson, T. Chem. Commun. 2013, 49, 8522; C.P. Bagowski, Y. You, H. Scheffler, D.H. Vlecken, D. J. Schmitz, I. Ott, Dalton Trans. 2009, 10799; K.J. Kilpin, C.M. Clavel, F. Edafe, P.J. Dyson, Organometallics 2012, 31, 7031; J.M. Perez, I. Lopez-Solera, E.I. Montero, M.F. Brana, C. Alonso, S.P. Robinson, C. Navarro-Ranniger, J. Med. Chem. 1999, 42, 5482; S. Roy, S. Saha, R. Mujumdar, R.R. Dighe, A.R. Chakravarty, Inorg. Chem. 2009, 48, 9501.

[12] E.E. Langdon-Jones, D. Lloyd, A.J. Hayes, S.D. Wainwright, H.J. Mottram, S.J. Coles, P.N. Horton, S.J.A. Pope, *Inorg. Chem.* **2015**, *54*, 6606; E.E. Langdon-Jones, N.O. Symonds, S.E. Yates, A.J. Hayes, D. Lloyd, R. Williams, S.J. Coles, P.N. Horton, S.J.A. Pope, *Inorg. Chem.* **2014**, *53*, 3788

[13] For example, A.J. Amoroso, M.P. Coogan, J.E. Dunne, V. Fernandez-Moreira, J.B. Hess, A.J. Hayes, D. Lloyd, C. Millet, S.J.A. Pope, C. Williams, Chem. Commun. 2007, 3066; A.W-T. Choi, M-W. Louie, S.P-Y. Li, H-W. Liu, B.T-N. Chan, T.C-Y. Lam, A.C-C. Lin, S-H. Cheng, K.K-W. Lo, Inorg. Chem. 2012, 51, 13289; A. Palmioli, A. Aliprandi, D. Septiadi, M. Mauro, A. Bernardi, L. De Cola, M. Panigati, Org. Biomol. Chem. 2017, 15, 1686; V. Fernandez-Moreira, M.L. Ortego, C.F. Williams, M.P. Coogan, M. D. Villacampa, M.C. Gimeno, Organometallics 2012, 31, 5950; E.E. Langdon-Jones, A.B. Jones, C.F. Williams, A.J. Hayes, D. Lloyd, H.J. Mottram, S.J.A. Pope, Eur. J. Inorg. Chem. 2017, 759; R.G. Balasingham, F.L. Thorp-Greenwood, C.F. Williams, M.P. Coogan, S.J.A. Pope, Inorg. Chem. 2012, 51, 1419; A.J. Amoroso, R.J. Arthur, M.P. Coogan, J.B. Court, V. Fernandez-Moreira, A.J. Hayes, D. Lloyd, C. Millet, S.J.A. Pope, New J. Chem. 2008, 32, 1097;

[14] K. de Oliveira, P. Costa, J. Santin, L. Mazzambani, C. Burger, C. Mora, R. Nunes, M. de Souza, Bioorg. Med. Chem. 2011, 19, 4295.
[15] L.A. Mullice, S.J.A. Pope, Dalton Trans. 2010, 39, 5908
[16] F.L. Thorp-Greenwood, M.P. Coogan, A.J. Hallett, R.H. Laye, S.J.A. Pope, J. Organomet. Chem. 2009, 694, 1400.
[17] Z.Y. Wu, J.N. Cui, X.H. Xian, T.Y. Liu, Chin. Chem. Lett. 2013, 24, 359
[18] M. Wrighton, D.L. Morse, J. Am. Chem. Soc. 1974, 96, 998

[19] http://www.molinspiration.com
[20] S.J. Coles, P.A. Gale, *Chem. Sci*., 2012, **3**, 683.
[21] *CrystalClear-SM Expert 3.1 b27*, 2013, Rigaku
[22] L. Palatinus, G. Chapuis, *J. Appl. Cryst*., 2007, **40**, 786.
[23] G.M. Sheldrick, *Acta Cryst*., 2015, **C71**, 3.